

# Statistical Shape Space Analysis Based on Level Sets

No Author Given

No Institute Given

**Abstract.** A framework for optimisation of specific criteria across the shape variability found in a population is proposed. The method is based on level set segmentation in the parametric space defined by Principal Component Analysis (PCA). The efficient narrow band evolution of the level set allows to search for the instances only in the neighborhood of the zero level set and not in the whole shape space. We are able to optimise any given criterion not to provide a single best fitting instance in the shape space, but rather to provide a group of instances that meet the criterion. This effectively defines a partition in the shape space, which can have any topology. The method works for data of any dimension, determined by the number of principal components retained. Results are shown on the application to shape analysis of human femora.

## 1 Introduction

Statistical shape analysis techniques enjoy a remarkable popularity in the medical image analysis community. Its flagship, the Active Shape Model (ASM), proposed by Cootes et al. [1] provides a method to study the structure of a population of point data sets or meshes, decomposing the variability encountered across the population in a compact representation. This decomposition is obtained via PCA [2].

Statistical shape models have been extensively used for image segmentation [1] and shape estimation from sparse sets of landmarks, e.g. for image-free computer assisted surgery [3]. In all these cases, the aim is to find the instance in the statistical shape model that best approximates the input data, subject to some regularisation constraints [3].

Optimisation in shape space of more complex criteria based on clinically meaningful shape measures related to anatomical locations has not been fully explored. Sierra et al. [4] formulate a minimisation process based on Lagrange multipliers to incorporate such additional constraints, and then optimise this criterion based on a gradient descent algorithm starting from the mean of the shape distribution. This is used in their application to generation of virtual anatomical models for surgery simulation, instantiated by specifying clinical parameters that depend non-linearly on the shape coefficients. However, their optimisation will only converge to a local minimum, which will not necessarily be the instance of the shape space that best meets the constraints.

Further, existing works aim at finding a single instance from the statistical shape model as the solution to their problem. In certain cases, it may be interesting to find *all* instances of the shape model that meet a certain criterion. For example, one may be interested in estimating which range of the population falls within a given anatomical criterion, thus establishing a partition of the shape space into “valid” and “invalid” shapes. To our knowledge, this is the first work that addresses this problem.

In this paper, we propose a method for global optimisation of shape constraints that effectively finds all instances in the PCA shape space that meet a given criterion. Our method is based on level set segmentation in the parametric shape space defined by PCA. Using the high dimensionality of level sets will allow for the segmentation of the space of any dimension, determined by the number of principal components retained. Moreover, the ability to represent the space with complex topologies can be used to identify disconnected subsets of the shape space that meet the criterion.

To avoid confusion, it should be mentioned that the combination of statistical shape models and level sets has been presented in previous works [5]. However, these works are of very different nature to ours, as they deal with the construction of statistical models of shapes represented by level sets (usually derived from distance maps). This is fundamentally different to the work presented in this paper.

Section 2 will briefly introduce the basic concepts behind statistical shape models based on PCA. Section 3 will present the level set formulation employed in our framework. In section 4 the key idea of this paper is introduced, that is, the use of level set segmentation in PCA shape space. Section 5 deals with initialisation and computationally efficient optimisation. In section 6 we illustrate our method by an application to anatomical studies. Finally, discussion and conclusions are provided in section 7.

## 2 Principal component analysis

PCA is a multivariate factor analysis technique aiming at finding a low-dimensional manifold in the space of the data, such that the distance between the data and its projection on the manifold is small [2]. PCA is the best, in the mean-square error sense, linear dimension reduction technique.

Given a set of training data  $\{\mathbf{t}_1, \mathbf{t}_2, \dots, \mathbf{t}_N\}$  in a given orthonormal basis of  $\mathcal{R}^D$ , PCA finds a new orthonormal basis  $\{\mathbf{u}_1, \dots, \mathbf{u}_D\}$  with its axes ordered. This new basis is rotated such that the first axis is oriented along the direction in which the data has its highest variance. The second axis is oriented along the direction of maximal variance in the data, orthogonal to the first axis. Similarly, subsequent axes are oriented so as to account for as much as possible of the variance in the data, subject to the constraint that they must be orthogonal to the preceding axes. Consequently, these axes have associated decreasing “indices”  $\lambda_d$ ,  $d = 1, \dots, D$ , corresponding to the variance of the data set when projected on the axes. The *principal components* are the set of new ordered basis vectors.

The way to find the principal components is to compute the sample covariance matrix of the data set,  $\mathbf{S}$ , and then find its eigenstructure

$$\mathbf{S}\mathbf{U} = \mathbf{U}\mathbf{A}$$

$\mathbf{U}$  is a  $D \times D$  matrix which has the unit length eigenvectors  $\mathbf{u}_1, \dots, \mathbf{u}_D$  as its columns, and  $\mathbf{A}$  is a diagonal matrix with the corresponding eigenvalues  $\lambda_1, \dots, \lambda_D$ . The eigenvectors are the principal components and the eigenvalues their corresponding projected variances.

### 3 Level set segmentation

Segmentation techniques based on active contours, or deformable models, have been widely used in image processing for different medical applications [6, 7]. The idea behind active contours is to extract the boundaries of homogeneous regions within the image, while keeping the model smooth during deformation. A particular instantiation of this paradigm is that of active contours based on level sets [8–12].

Let us consider a parameterized closed surface  $C(s) : S = [0, 1]^{D-1} \rightarrow \mathcal{R}^D$  defined in a bounded region  $\Omega \in \mathcal{R}^D$ . In order to segment the observed image  $\mu : \Omega \rightarrow \mathcal{R}$  we propose to minimize the following energy functional:

$$E(C) = a \int_{\omega} (\mu - M) dx + b \int_S |C'| ds, \quad (1)$$

where  $\omega \subset \Omega$  and  $C = \partial\omega$  is the region inside the curve. The first term represents the boundary force that attracts the evolving curve towards a predefined segmentation constraint  $M = \text{const}$ , while the second term regulates the smoothness of the curvature.  $a$  and  $b$  are scalar weights.

The proposed energy functional is not easy to solve because of the unknown set of complex contours  $C$  and unidentified image topologies. The segmentation algorithm developed in this work is based on the implicit representation of deformable models implemented within the framework of level sets. This implicit representation for evolving curves, introduced by Osher and Sethian [13], allows automatic change of topologies without re-parametrization. Using the level set formulation, the boundary contour  $C = \partial\omega$  can be modelled as a zero level set of a Lipschitz function  $\phi$ , defined on the entire image domain  $\Omega$  as:  $\phi(x) > 0$  *inside*  $C = \omega$ ,  $\phi(x) = 0$  on  $C = \partial\omega$  and  $\phi(x) < 0$  *outside*  $C = \Omega \setminus \omega$ .

Having the Heaviside function  $H(\phi)$  defined on the whole image domain and its corresponding Dirac function  $\delta(\phi) = \frac{d}{d\phi}H(\phi)$ , we can replace the unknown variable  $C$  by the level set function  $\phi(x)$  as:

$$E(\phi) = a \int_{\Omega} (\mu - M) H(\phi) dx + b \int_{\Omega} \delta(\phi) |\nabla(\phi)| dx, \quad (2)$$

where the curvature value  $|C(\phi = 0)| = \int_{\Omega} \delta(\phi) |\nabla(\phi)| dx$  is estimated directly from the level set function [14]. By minimizing the energy functional with respect

to  $\phi$  we get a model associated Euler-Lagrange equation for boundary flow:

$$\frac{\partial \phi}{\partial t} = a(\mu - M)\delta(\phi) + b \operatorname{div}\left(\frac{\nabla \phi}{|\nabla \phi|}\right)\delta(\phi). \quad (3)$$

#### 4 Optimisation in PCA shape space using level sets

Let us consider the shape space defined by the weighted linear combination of the first  $L \leq D$  eigenvectors  $\mathbf{u}_1, \dots, \mathbf{u}_L$  of the PCA decomposition of a set of training shapes in  $\mathcal{R}^D$ . Each element  $m \in \mathcal{R}^D$  in this shape space is defined by a set of coefficients  $\alpha_1, \dots, \alpha_L$ :

$$m = \bar{m} + \sum_{i=1}^L \alpha_i \sqrt{\lambda_i} \mathbf{u}_i, \quad (4)$$

where  $\lambda_1, \dots, \lambda_L$  are the eigenvalues corresponding to each principal component, and  $\bar{m}$  is the arithmetic mean of the training sets (Figure 1).

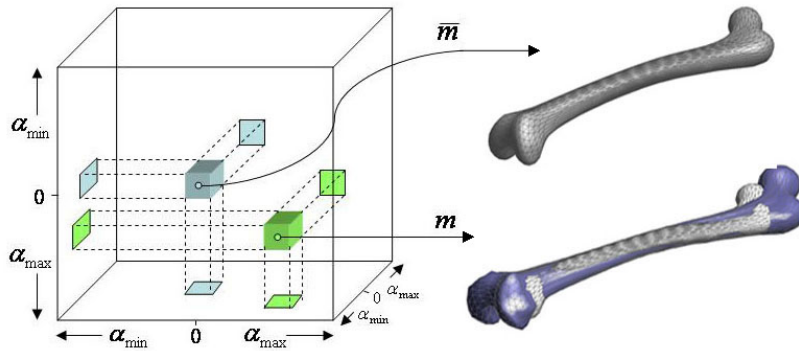


**Fig. 1.** Shape space defined by the three first principal components. The center element (labelled in the figure  $\bar{m}$ ) corresponds to the mean of the population. Each element in this shape space is formed by a linear combination of the principal components, in this case  $m = \bar{m} + \alpha_1 \sqrt{\lambda_1} \mathbf{u}_1 + \alpha_2 \sqrt{\lambda_2} \mathbf{u}_2 + \alpha_3 \sqrt{\lambda_3} \mathbf{u}_3$ .

Now let us consider a scalar mapping  $\mathcal{M} : A = [\alpha_{\min}, \alpha_{\max}]^L \rightarrow \mathcal{R}$ . This mapping represents a clinically meaningful anatomical criterion derived from the shapes in the PCA shape space. We now would like to find all instances in the shape space that meet a certain criterion dependent on the scalar measure  $M$ . This problem is approached as a segmentation in the space defined by the mapping  $\mathcal{M}$  defined above, and solved using the level sets framework described in section 3. Thus, adopting the nomenclature of the previous section,  $\mu = \mathcal{M}$  will be the  $L$ -dimensional “image”  $\mu$  to be segmented, defined in the domain of shape coefficients  $\Omega = A$ . An illustrative example is shown in section 6; the following section addresses computational efficiency.

## 5 Computational issues

In order to decrease the computational complexity of the standard level set method we apply a *narrow band level set* approach, which uses only the points close to the evolving front at every time step [15, 16]. First we initialize a thin band around the zero-level set, that contains the neighboring points with distance to the zero-level less than  $d_{max}$  and we update the level set only on these points, instead of re-calculating it for each grid point. As the zero-level set corresponding to the front evolves, we must ensure that it stays within the band. We re-initialize the band when the front is close to the edge of the domain, using the current zero-level set as the initial surface.

We initialize our level set function using *automatic seed initialization* and then iteratively evolve the curve toward the segmented region by minimizing the energy functional. The seed initialization consists of partitioning the data image  $\mu$  into  $N$   $L$ -dimensional windows  $W_{n,n=1..N}$  of predefined size. Then we initialize the corresponding circular signed distance on each  $L$ -dimensional window  $W_n$ .

## 6 Results

We present results obtained from a training set of 30 surface models extracted from CT data. These models represent complete left human femurs. Correspondences across data sets were established with a spherical harmonic (SPHARM) based shape representation method [17]. These correspondences are further optimized via a Minimum Description Length (MDL) optimization [18]. The average shape was computed by simple averaging of corresponding landmarks across the data sets. The remaining variation was analyzed by PCA (Figure 2).

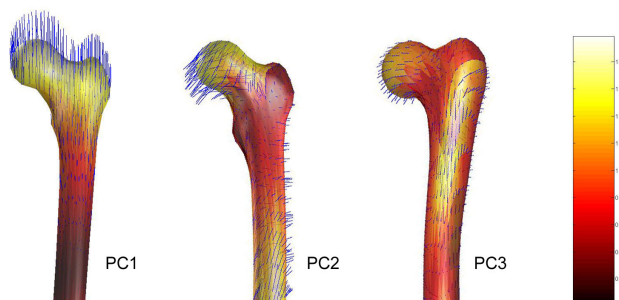


**Fig. 2.** First three modes of variation for left femur. The lines represent the positive direction of of the principal component (PC). The first mode describes the change of the femur length, second mode is responsible for the inclination of the femoral head and the third mode describes a deformation of the posterior part of the femoral head and a slight torsion and curvature of the central region.

We retain the first three principal components  $u_1$ ,  $u_2$  and  $u_3$ , which account for 89.22% of shape variability in the population. This will allow us to explain and visualize each step of the method as 3D images, although it can be applicable to data of any dimension. The shape space is thus built by sampling the space of shape coefficients, generating the corresponding shape, and then computing the mapping  $M$  to obtain the measure of interest. In this case, we use the range  $-3 \leq \alpha_i \leq 3$  for every shape coefficient. This accounts for 99.7% of the shape variability encompassed in each principal component.

The clinical measure of interest  $\mathcal{M}$  in our example, defined as:

$$FIA(\alpha_1, \alpha_2, \alpha_3) = \frac{1}{F} |ang(\bar{m}) - ang(m)|, \quad (5)$$

represents the difference between the angle of femoral stem implant and the angle of femoral inclination (FI) of the generated instance mesh, where  $F$  is normalization factor. Femoral inclination is defined as frontal plane alignment of femoral head and neck relative to shaft, and is commonly employed in clinical practice as a descriptive parameter (Figure 3). In normal adults, the neck of the femur forms an angle of from  $126^\circ$  to  $128^\circ$  with the shaft and any big variation from this value results in hip deformations [19].

We generate our scalar 3D map by computing FIA values, and the obtained range of femoral inclination angles from  $125.5^\circ$  to  $145.6^\circ$  correlates well with previous studies [20]. We compute the set of the bones that have  $127^\circ$  neck angles, as designed for Omnifit EON femoral stem implant by Stryker Orthopaedics. As discussed in the previous section, we do not need to explicitly compute  $M$  for every point in the shape space, but only in a narrow band around the zero level set. The segmented area represents the range of parametric values that generate femur shapes that have a similar range of the femoral inclination  $127^\circ \pm 2.5^\circ$  (Figure 4).

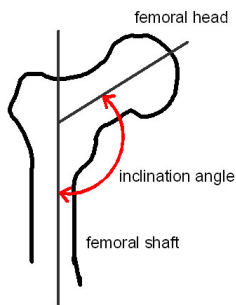


**Fig. 3.** Femoral inclination angle is chosen to fit the Omnifit EON femoral stem implant designed by Stryker with offset  $127^\circ$ .

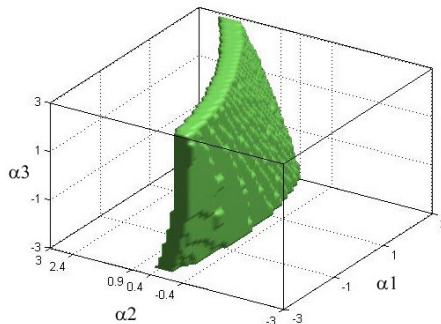


**Fig. 4.** Automatic 3D level set segmentation gives the spectrum of shapes that have femoral inclination  $127^\circ \pm 2.5^\circ$ .

It can be seen in Figure 5 that the second principle component mostly affects the value of the femoral inclination and that the spectrum of segmented shapes moves toward the greater variation of the first and third principle component. These results can also be of high importance in the field of femoral stem design, and can lead to choosing the representative parameters that would yield to the implant shape that best fits the populations.

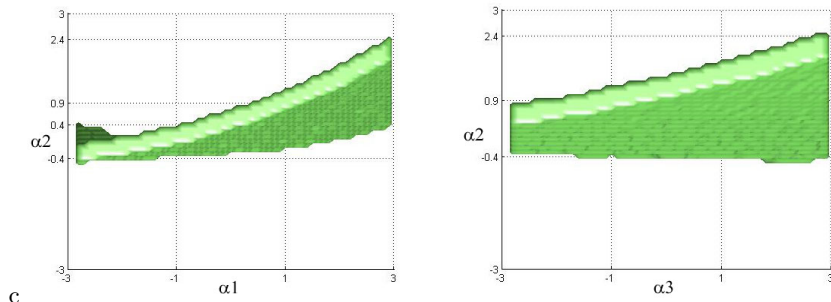


**Fig. 5.** 2D maps are showing the segmented spectrum of shapes and its high dependence on the second principle component.

In our numerical experiments, we use the Cauchy distribution to approximate Heaviside  $H_\varepsilon(\phi)$  and Dirac  $\delta_\varepsilon(\phi) = H'_\varepsilon(\phi)$  functions:  $H_\varepsilon(\phi) = \frac{1}{2}(1 + \frac{2}{\pi} \text{atan}(\phi))$ . The initialization of a zero level set is done using automatic seed initialization with 64 windows of radius equal to 4, equidistantly distributed on the shape space domain. The narrow band contains the neighboring points with distance to the zero-level less than  $d_{max} = 4$ . Reinitialization of the narrow band is done after every 10 iterations.

## 7 Discussion

In this paper we have proposed a framework for optimisation in PCA shape space based on level sets. The method allows to find a partition of the shape distribution into regions that meet / do not meet a given criterion. Illustrative results have been shown for anatomical analysis of femur bone. Although the example has been elaborated for 3D maps (i.e. taking only 3 principal components), the method is applicable to maps of any dimension and topology.

To our knowledge, this is the first research into the problem of finding all instances in a shape distribution meeting a given criterion. The practical use of such a concept is of extreme importance in the study of the anatomical evidence of a pathology, or the morphologic features in implant design. Ongoing work includes the application of the proposed method to bone implant fitting assessment taking into account shape and biomechanical properties of a combined shape and intensity statistical bone model.

## References

1. T.F. Cootes, C.J. Taylor, D.H. Cooper, and J. Graham, "Active shape models - their training and applications," *Comp. Vis. Image Underst.*, vol. 61, no. 2, 1995.
2. C. Bishop, *Neural Networks for Pattern Recognition*, Oxford Univ. Press, 1995.
3. Anonymized
4. R. Sierra, G. Zsemlye, G. Szekely, and M. Bajka, "Generation of variable anatomical models for surgical training simulators," *Medical Image Analysis*, vol. 10, no. 2, pp. 275–285, 2006.
5. M. Leventon, W.E.L. Grimson, O. Faugeras, and W.M. Wells, "Level set based segmentation with intensity and curvature priors," in *Proceedings of IEEE Workshop on Mathematical Methods in Biomedical Image Analysis*, 2000.
6. M. Kass, A. Witkin, and D. Terzopoulos, "Snakes: Active contour models," *Int. Journal of Computer Visualisation*, vol. 1, pp. 321–331, 1980.
7. T. McInerney and D. Terzopoulos, "Deformable models in medical images analysis: a survey," *Med. Image Analysis*, vol. 1, no. 2, pp. 91–108, 1996.
8. D. Mumford and J. Shah, "Optimal approximation by piecewise smooth functions and associated variational problems," *Comm. on Pure and Applied Mathematics*, vol. 42, pp. 577–685, 1989.
9. T.F. Chan and L.A. Vese, "Active contours without edges," *IEEE Trans. on Image Processing*, vol. 10, pp. 266–277, 2001.
10. X.F. Chen and Z.C. Guan, "Image segmentation based on mumford-shah functional," *Journal of Zhejiang University SCIENCE*, vol. 5, pp. 123–128, 2004.
11. A. Tsai, A. Yezzi, and A.S. Willsky, "Curve evolution implementation of the mumford-shah functional for image segmentation - denoising, interpolation, and magnification," *IEEE Trans. on Image Processing*, vol. 10, pp. 1169–1186, 2001.
12. H.-K. Zhao, T. Chan, B. Merriman, and S. Osher, "A variational level set approach to multiphase motion," *J. of Computational Physics*, vol. 127, pp. 179–195, 1996.
13. S. Osher and J.A. Sethian, "Fronts propagating with curvature-dependent speed: Algorithms based on hamilton-jacobi formulation," *Journal on Computational Physics*, vol. 79, pp. 12–49, 1988.
14. L.C. Evans and R.F. Gariepy, *Measure Theory and Fine Properties of Functions*, Boca Raton, FL: CRC, 1992.
15. D. Adalsteinsson and J.A. Sethian, "A fast level set method for propagating interfaces," *Journal of Computational Physics*, vol. 118, pp. 269–277, 1995.
16. C. Li, C. Xu, K.M. Konwar, and M.D. Fox, "Fast distance preserving level set evolution for medical image segmentation," in *ICARCV*, 2006.
17. C. Brechbühler, G. Gerig, and O. Kübler, "Parametrization of closed surfaces for 3-d shape description," *Comp. Vis. Image Underst.*, vol. 61, pp. 154–170, 1995.
18. R.H. Davies, C.J. Twining, T.F. Cootes, J.C. Waterton, and C.J. Taylor, "A minimum description length approach to statistical shape modelling," *IEEE Trans. on Medical Imaging*, vol. 21, no. 5, pp. 525–537.
19. W. Platzer, W. Kahle, and M. Frotscher, *Color Atlas and Textbook of Human Anatomy: Locomotor System*, Thieme Medical Publishers, 2004.
20. Anonymized